JOM, Vol. 76, No. 7, 2024
https://doi.org/10.1007/s11837-024-06566-7

Phase Transformation Law of Manganese and Iron Oxides in Ferromanganese Ore During Gas-Based Simultaneous Reduction Roasting

MENG-FEI LI,[1] HAN-QUAN ZHANG,[1] XIN XU,[2] and MAN-MAN LU [1,3]

1.—School of Resources and Safety Engineering, Wuhan Institute of Technology, Wuhan 430073, Hubei, China. 2.—WISCO Resources Group Chengchao Mining Company Limited, Ezhou 436051, China. 3.—e-mail: lummwit@wit.edu.cn

Manganese is widely used in the iron and steel industry, batteries and other fields. The amount of the manganese oxide ores existing in China coeval with iron and their manganese-to-iron ratio is low. A study was conducted on a synchronous reduction roasting-magnetic separation of a ferromanganese ore with high content of iron taken from South Africa using CO as reductant. Under the conditions of 750°C roasting temperature, 40 min roasting time, 30% CO concentration roasting atmosphere and − 0.074 mm accounting for 82.56% grinding fineness, the iron removal rate was close to 70% through magnetic separation, with the grade and manganese recovery of manganese concentrate reaching 49% and 72.50% and the manganese-to-iron ratio increasing from 2.5 to 5.92. The X-ray diffraction analysis indicated that Mn_2O_3 and Fe_2O_3 in the raw ore was reduced to MnO and Fe_3O_4, respectively, without forming the intermediate product Mn_3O_4 in a weak reducing atmosphere. The SEM-EDS analysis of the roasted product showed that the simultaneous reduction of manganese and iron oxides could be achieved when the roasting temperature reaches 750°C. The crystal forms of MnO and Fe_3O_4 were more perfect, and the coexisting grains of Ca, Si and Al clustered further with increasing roasting temperature.

INTRODUCTION

Manganese (Mn) plays a very important role in all fields of the national economy, and it is one of the most abundant chemical elements on the earth.[1] With numerous applications in non-ferrous metallurgy, building materials, electronic materials, environmental protection, chemical industry, light industry and other fields, manganese is usually used as a deoxidizer, desulfurizer and additive in manganese ferroalloys.[2–4] Manganese is also widely used in the steel industry, with the saying that "no steel without manganese."[5,6] Therefore, utilizing complex manganese ore resources is important.

China is a manganese-rich country in terms of reserves, with 900 million tons of proven manganese reserves and 44 million tons of metal quantities, ranking sixth in the world. However, China is also a country with poor manganese resources in terms of resource endowment.[7] Figure 1 shows the manganese resources in China are mainly distributed in Guangxi, Yunnan, Hunan, Guizhou and Sichuan, accounting for about 90% of the total manganese reserves in China. Manganese ores existing in China are low grade, with a fine embedded particle size and many impurity elements. The average grade of manganese ore in China is only 21%, far below the requirement for international commercial grade manganese ore.[8–10] Considering the domestic manganese ore with low grade and limited reserves, which cannot meet the demand, a large amount of manganese ore must be imported from abroad, with South Africa being the main importer of manganese ore to China.

(Received November 23, 2023; accepted April 2, 2024; published online April 29, 2024)

The main type of manganese ore in China is ferromanganese, which can be utilized after pre-separation and beneficiation. However, obtaining better beneficiation effect through single gravity separation, magnetic separation or flotation separation processes is difficult. Normally, some combined processes including physical sorting (gravity separation, magnetic separation and flotation separation) and chemical treatment are used to separate the iron and manganese components in ferromanganese ore.[11] On the other hand, the manganese in these ores is in the form of Mn^{+4} (MnO_2) or Mn^{+3} (Mn_2O_3), which is difficult to leach out without a reducing. The pre-treatment of raw ores using gravity separation, magnetic separation and flotation processes can remove some impurities, making the subsequent chemical treatment of flotation products achieve better separation and recovery effects.[12–15]

At present, chemical methods primarily include the direct reduction-leaching process, pre-reduction roasting-leaching process and pre-reduction roasting-magnetic separation process.[16] The direct reduction leaching process, which can obtain a high leaching rate, is suitable to separate low-grade pyrolusite, but the reaction rate is low.[17,18]

The most common process to separate the ferromanganese ore with high iron content is the reduction roasting-magnetic separation-leaching method, reducing the mixing of iron impurities in the leaching process and making full use of iron and manganese component. Currently, research has shown roasting a ferromanganese ore for 20–40 min using CO or coal as reductant at 600–650°C; most MnO_2 and Fe_2O_3 in the raw ore were reduced to MnO and Fe_3O_4, respectively; the leaching rate of manganese was > 82.37%, and the leaching rate of iron was controlled to be < 7% by acid leaching. X-ray diffraction analysis showed that most MnO_2 and Fe_2O_3 in the raw ore were effectively reduced to MnO and Fe_3O_4.[19,20]

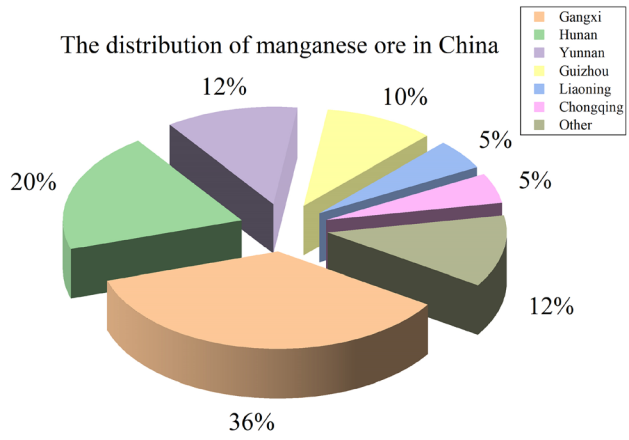

Fig. 1. Distribution of manganese ore in China.

Research interest in ferromanganese ore has arisen, considering the importance and large utility of both Fe and Mn.[21] In this research, the reduction roasting-magnetic separation process was used in the raw ore to investigate the beneficiation route of iron-rich manganese ore. The raw ore was roasted in a reducing atmosphere, making the high valence iron manganese oxide reduce to a low valence state.[22] Subsequently, the iron and manganese components were separated through magnetic separation to recover a valuable iron bearing byproduct (magnetite concentrate) and manganese ore concentrate for ferroalloy production process using ferromanganese ores. The X-ray diffraction and SEM-EDS analyses were used to analyze the iron and manganese phase transformation during the reduction roasting process. The main purpose of this research is to find out the details during the reduction roasting process of iron-rich manganese ore under different thermodynamic conditions and explore methods to significantly increase the manganese-to-iron ratio.

MATERIALS AND METHODS

Raw Materials

The raw ore sample was obtained from South Africa. The ore which was used in the experiments has been processed into − 2 mm through jaw fracture and roller alignment. First, the multielement analysis was performed to ascertain the main chemical composition of the ferromanganese ore. The result is shown in Table I.

The dominant content of manganese and total iron were 40.90% and 16.36%, respectively. The manganese-to-iron ratio was 2.5. The gangue minerals were primarily siliceous and calcium-bearing minerals. The relatively high contents of SiO_2 and CaO were 4.58% and 7.21%, respectively. Figure 2 shows the detailed spectrum of XRD to determine the main phase composition in the raw ore.

The figure shows that the phase of manganese in the raw ore consisted of a large part of manganese trioxide and a small amount of ferromanganese oxide. The occurrence form of iron minerals was

Table I. Analytical results of the main chemical composition of the raw ore/%

TMn	TFe	Al_2O_3	SiO_2	CaO	MgO	Loss on ignition
40.90	16.36	0.3	4.58	7.21	0.76	6.52

hematite, and the main gangue mineral was quartz. Table II lists the results of sieve analysis tests through wet screening to determine the distribution of manganese and iron in each class size.

The table shows that the manganese grade decreased with the particle size decreasing, with 36.26% the lowest grade at − 0.043 mm fraction. Over 75% of the particles were > 0.3 mm, and < 0.3 mm were a small part. Iron grades of particles > 0.9 mm and < 0.075 mm were higher, and iron was primarily distributed in the coarse particles. The distribution of iron in the raw ore was relatively uniform, while the manganese grade in the coarse particles was higher than that in the fine particles. The manganese grade became lower with decreasing particle size, making screening an infeasible process option for processing this ore. SEM-EDS was used to study the distribution characteristics of minerals and the compositions of the raw ore by observing the microstructure and EDS spectrum, as shown in Fig. 3.

Three main phase compositions in the raw ore could be seen in Fig. 3. The gray grains primarily contained Mn, O and a small amount of Fe. The gray-white crystals in the middle and edge of the mineral contained high contents of Fe, Mn and O. Combined with X-ray diffraction, the phase of manganese was primarily Mn_2O_3 and a small amount of other ferromanganese oxides. The phase of iron was primarily hematite, but most of it was mixed with ferromanganese oxide, making it difficult to separate manganese oxide and iron oxide completely. Some black particles could be seen, indicating that the oxides of impurity elements such as Ca and Si concentrated together. X-ray diffraction analysis shows that the minerals of these impurity elements would be closely combined with manganese oxide, and they might enter manganese concentrate with manganese oxide in the separation process.

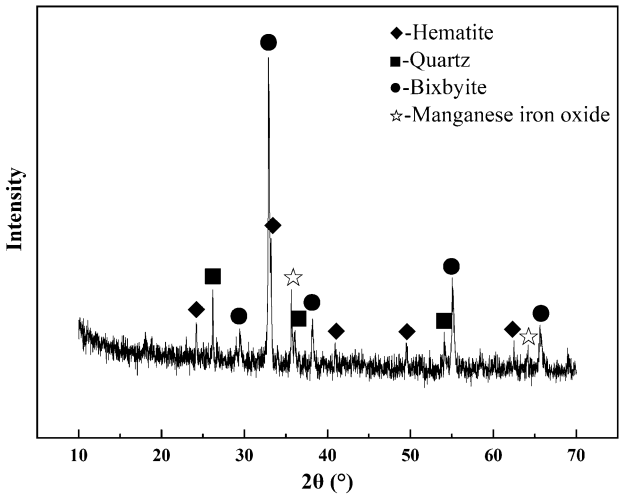

Fig. 2. XRD spectrum of high iron manganese oxide ore.

Experimental Method

The experiments in this study (from Fig. 4) included the magnetization roasting of the raw ore, grinding, magnetic separation of the roasted samples and describing the products.

Experimental Process

The gas-based reduction roasting experiment was performed in a tube furnace (GSL-1400X, primarily exploring the influence of roasting temperature, roasting time and other parameters on the reduction effect. After grinding the roasted ore, magnetic product containing Fe_3O_4 and non-magnetic product containing MnO were separated through a Davis tube unit, with a 28.26 kA/m magnetic field intensity. Chemical titration was used to measure the grade and recovery of Fe and Mn. X-ray diffraction analysis on roasted ores under different roasting temperatures and roasting times was performed, and the relative content of iron and manganese oxides was determined through data fitting method. The experimental process is shown in Fig. 4.

Reduction roasting process

Carbon monoxide is commonly used as a reducing agent during gas-based reduction roasting and the chemical reactions are as follows:

$$3Fe_2O_3 + CO(g) = 2Fe_3O_4 + CO_2(g)$$
$$\Delta G^{\theta} = -42.282 - 0.056T \quad (1)$$

Table II. Yield, grade and distribution rates of manganese and iron by grain size of manganese ore/%

Particle size	Productivity/ %	TFe/ %	TMn/ %	Fe distribution law (mass fraction)	Mn distribution law (mass fraction)
+ 0.9 mm	55.82	16.72	41.78	57.06	56.93
− 0.9 + 0.3 mm	20.59	15.50	40.73	19.51	20.47
− 0.3 + 0.15 mm	9.97	15.54	40.62	9.47	9.89
− 0.15 + 0.075 mm	3.34	15.76	40.18	3.22	3.28
0.075 + 0.043 mm	3.83	17.10	39.94	4.00	3.73
− 0.043 mm	6.45	17.08	36.26	6.74	5.70
Total	100.00	16.36	40.96	100.00	100.00

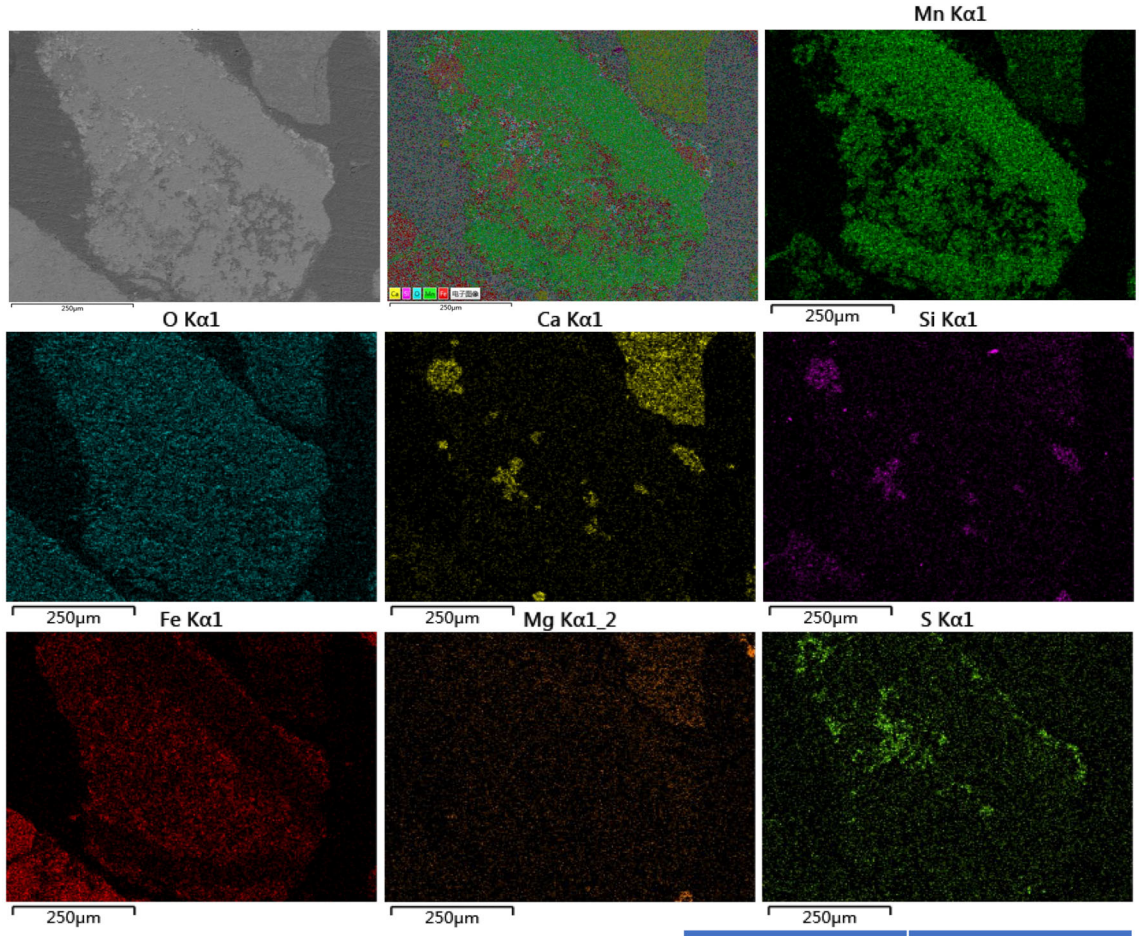

Element	Atomic percent / %
O	42.94
Mn	36.71
Fe	14.84
Si	1.64
Ca	2.81
Mg	1.06
Total	100.00

Fig. 3. Surface scan and EDS spectrum of high iron manganese oxide ore.

$$3Mn_2O_3 + CO(g) = 2Mn_3O_4 + CO_2(g) \quad \Delta G^{\theta} = -182.629 + 0.008T \tag{2}$$

$$Mn_3O_4 + CO(g) = 3MnO + CO_2(g) \quad \Delta G^{\theta} = -52.368 - 0.034T \tag{3}$$

The calculated standard Gibbs free energy of three reactions is shown in Fig. 5. As shown in Fig. 5, three reactions can occur spontaneously when the temperature exceeds 273.15 K. Moreover, Fe_2O_3 and Mn_3O_4 are more easily reduced by CO with increasing roasting temperature.

CO gas was used as the reducing gas, and N_2 gas was used as the protective gas in the gas-based roasting experiment. Fifty grams of the raw ore was pressed and placed in a reaction porcelain boat. Before reduction, N_2 was pre-introduced into the furnace until all air was displaced. Then we started

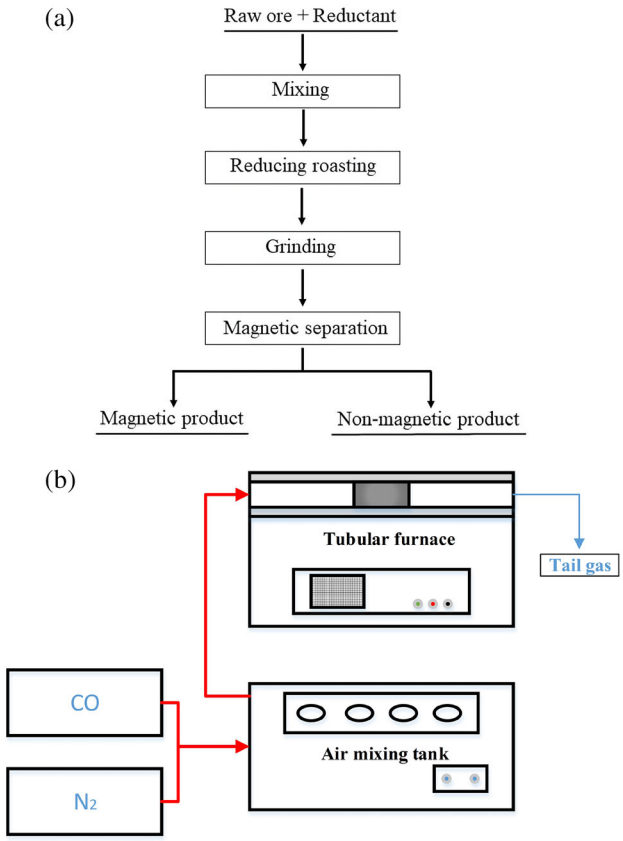

Fig. 4. Experimental process and schematic diagram of the gas-based reduction roasting unit: (a) experimental flow of gas-based reduction roasting-magnetic separation of high iron manganese oxide; (b) schematic diagram of the gas-based reduction roasting unit for manganese oxide ore.

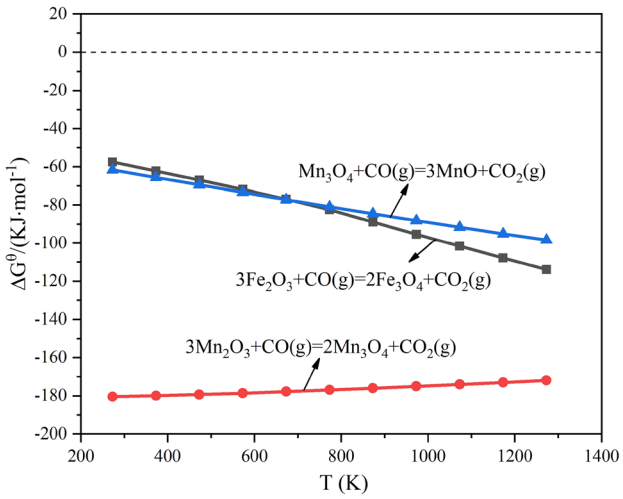

Fig. 5. Relationship between Gibbs free energy and temperature in CO reduction of iron and manganese oxides.

the temperature control program and set parameters of roasting temperature, roasting time and reducing gas concentration. After roasting, the roasted ore was cooled to room temperature under an N_2 atmosphere.

RESULTS AND DISCUSSION

Roasting Experiments

Effect of Particle Size on Reduction

The particle size of the raw ore has a very important impact on the roasting effect. The raw ore with too fine particle size makes gaseous reducing agents diffuse slowly and the internal particles reduce insufficiently, leading to poor quality of the roasting products. The raw ore with too large particle size makes the permeability of the material poor and the coming into contact of reducing gases with the internal particles difficult, resulting in insufficient reduction.[23] Therefore, studying the particle size of the raw ore on the roasting effect is of great significance. The raw ore was crushed to different particle sizes through grinding, and CO concentration (volume fraction) was controlled to 30% for 60 min at a roasting temperature of 750°C. The magnetic separation results of the roasted ore are shown in Fig. 6.

As shown in Fig. 6, the manganese grade of the non-magnetic product (manganese concentrate) decreased with particle size of the raw ore decreasing, and the manganese recovery initially decreased and then increased. The iron grade of the iron concentrate initially increased and then decreased with decreasing particle size, and the recovery rate of iron initially decreased and then increased. The iron recovery of the magnetic product was the highest when the particle size was 0–1000 μm, reaching 34.25% with 44.99% the iron grade. The manganese grade and manganese recovery of the non-magnetic product were 48.22% and 92.58% under this condition, respectively. The manganese-iron ratio of the manganese concentrate increased from 2.5 to 3.48. Considering the recovery of iron and manganese, the optimal particle size was determined to be 0–1000 μm.

Effect of Reducing Temperature

The main factors affecting the reduction of manganese oxide and iron oxide are roasting temperature, roasting time and reduction atmosphere. The properties of product and the degree of reaction are determined to some extent by roasting temperature during reducing roasting. With a controlled roasting time of 60 min and a CO content of 30%, the experiment results of the effect of roasting temperature on the reduction of manganese and iron oxides are shown in Fig. 7.

As shown in Fig. 7, the iron grade of the magnetic separation concentrate decreased with increasing roasting temperature, and the iron recovery initially increased and then decreased. The manganese grade of the magnetic separation tailings (manganese concentrate) initially increased and then decreased. The iron grade of the iron concentrate was 44.99% with the highest recovery of 34.25% at a

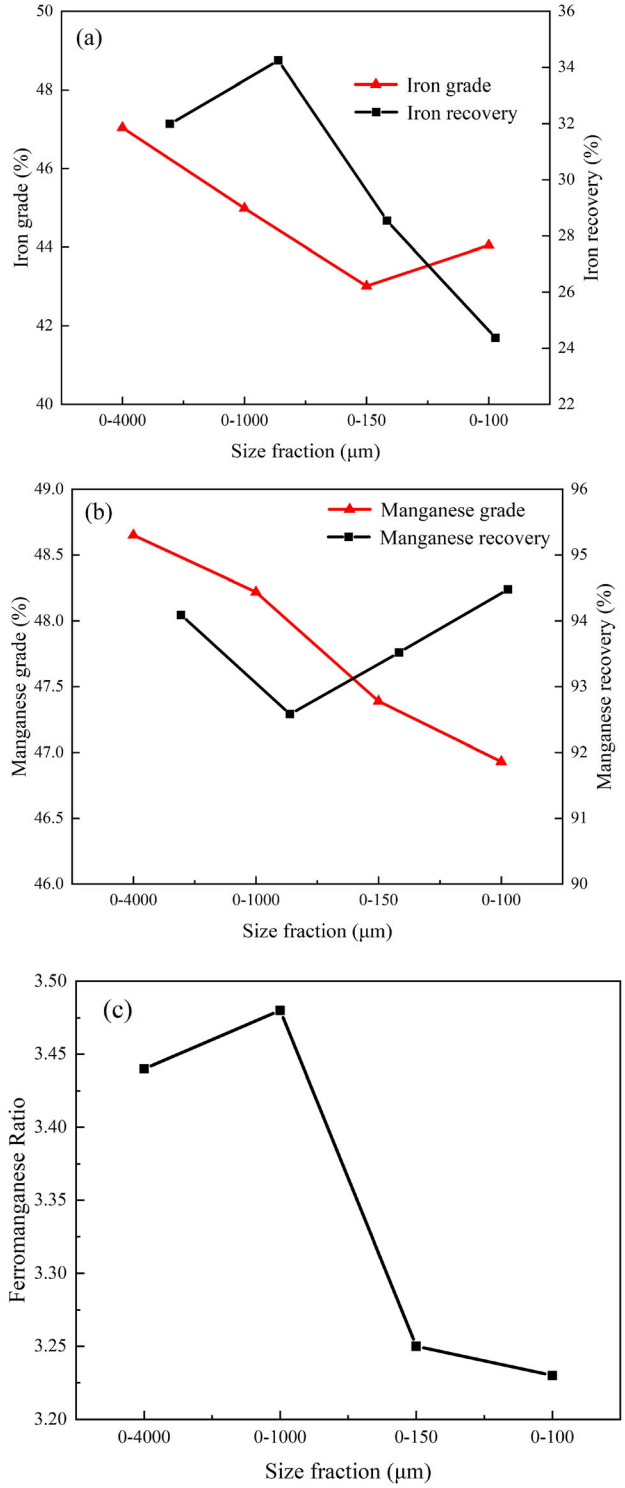

Fig. 6. Influence of ore particle size on roasting of manganese oxide ore: (a) iron concentrate; (b) manganese product; (c) ratio of manganese to iron.

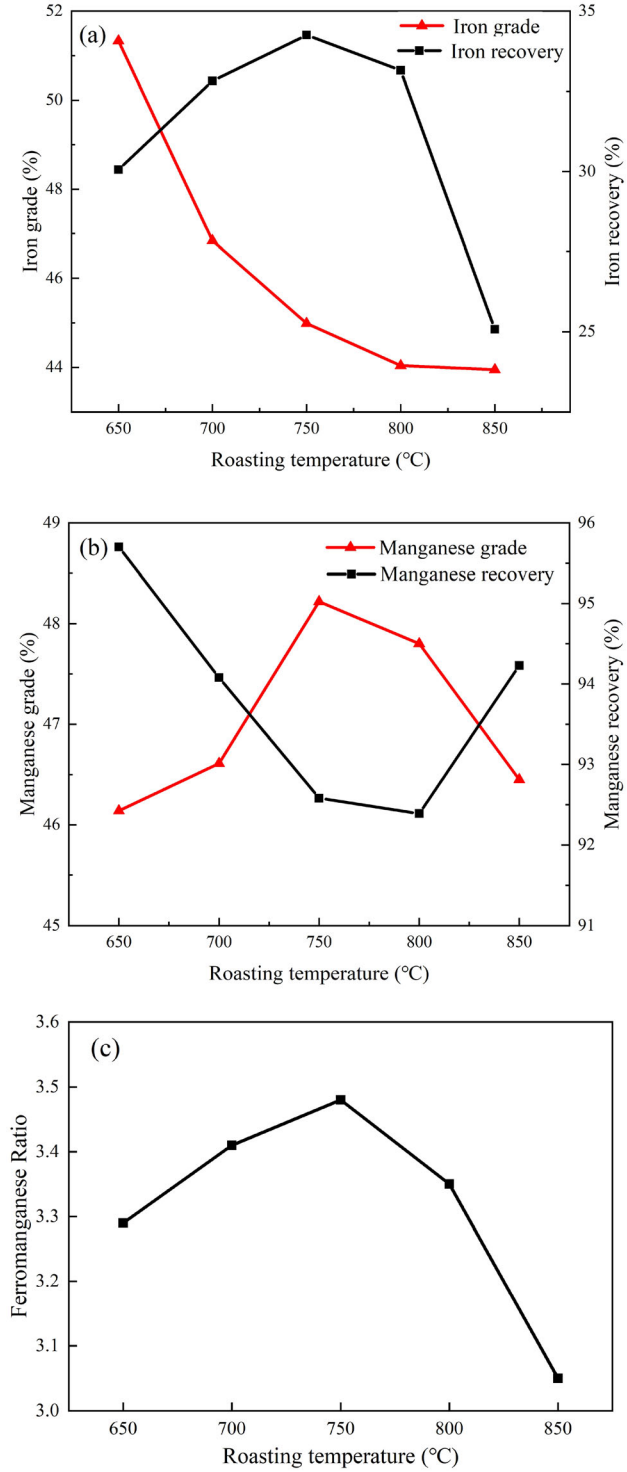

Fig. 7. Influence of roasting temperature on of manganese oxide ore: (a) iron concentrate; (b) manganese separation; (c) ratio of manganese to iron.

roasting temperature of 750°C. The manganese grade of the manganese concentrate was 48.22% with a 92.58% manganese recovery, and the manganese iron ratio was increased from 2.5 to 3.48.

The figure shows that hematite could not convert into magnetite completely when the roasting temperature was < 750°C, resulting in the decline of iron recovery. Part of the regenerated magnetite underwent overreduction when the roasting temperature was > 750°C,[24–26] and some wüstite

remaining in non-magnetic minerals decreased the manganese grade and manganese-to-iron ratio. The optimal roasting temperature was determined to be 750°C.

Effect of Roasting Time

The roasting time is also one of the important factors determining reduction roasting. Extremely long roasting time will cause energy waste and "overreduction," while excessively short roasting time will lead to an insufficient reaction called "under reduction."[27,28] The roasting temperature and CO concentration were controlled at 750°C and 30%, respectively. The experimental results of the influence of roasting time on the reduction of manganese oxide and iron oxide are shown in Fig. 8.

As shown in Fig. 8, prolonging roasting time was beneficial to iron reduction. The iron grade of the iron concentrate continuously rose, and the iron recovery initially increased and then decreased with the extension of roasting time. However, long roasting time might lead to overreduction of Fe_3O_4. The manganese grade of the manganese concentrate initially increased and then decreased with the prolonging of roasting time, and the manganese recovery initially decreased and then increased. The iron grade and iron recovery of the magnetic concentrate were 40.02% and 46.61%, respectively, when the roasting time was 40 min. The manganese grade and manganese recovery of the manganese concentrate were 47.96% and 86.49%, and the manganese-to-iron ratio increased from 3.48 to 3.99. Considering the simultaneous reduction separation of iron and manganese, the roasting time was determined to be 40 min.

Influence of CO Concentration

An experimental study of the effect of CO concentration on the reduction of manganese and iron oxides was performed at a roasting temperature of 750°C and roasting time of 40 min. Low CO concentration may lead to insufficient reduction, while with high CO concentration overreduction easily occurs, resulting in the formation of wüstite and reducing the recovery rate of iron. A study showed that the grades and recovery rates of iron and manganese were higher when CO concentration was 10–40 vol.%.[29] Therefore, 10–40 vol.% CO as reducing gas with 90–60 vol.% N_2 as protective gas was chosen in this experiment. The influence of the CO concentration on the magnetic separation products is listed in Fig. 9. Due to the low yield of the previous magnetic separation concentrate and a high iron content in the manganese concentrate, the manganese concentrate was scavenged using a 46.33 kA/m magnetic field intensity.

As shown in Fig. 9, the iron grade of the magnetic separation concentrate initially decreased and then increased with the increase of CO concentration (v/v%), and the iron recovery initially increased and

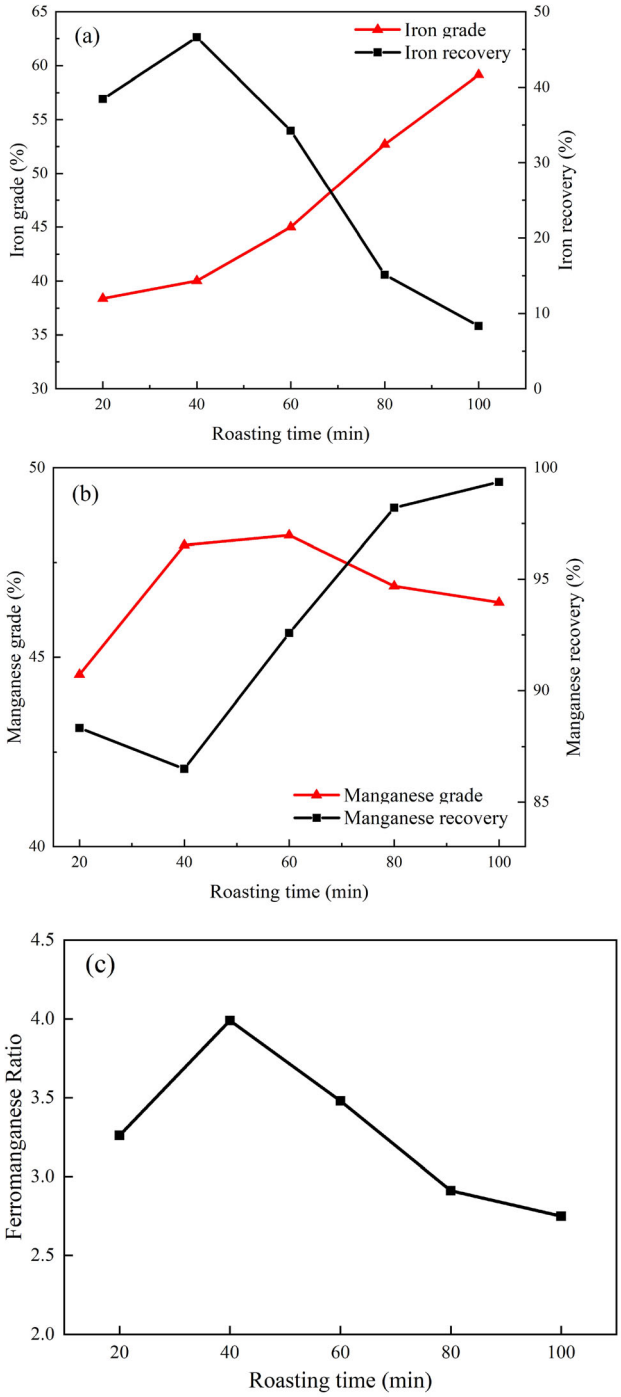

Fig. 8. Influence of roasting time on roasting of manganese oxide ore: (a) iron concentrate; (b) manganese separation; (c) ratio of manganese to iron.

then decreased. The manganese grade of the non-magnetic products increased with the increase of CO concentration, and the manganese recovery initially decreased and then increased. The iron grade and iron recovery of the iron concentrate were 40.02% and 46.60%, respectively, under the condition of 30% CO concentration. The manganese grade

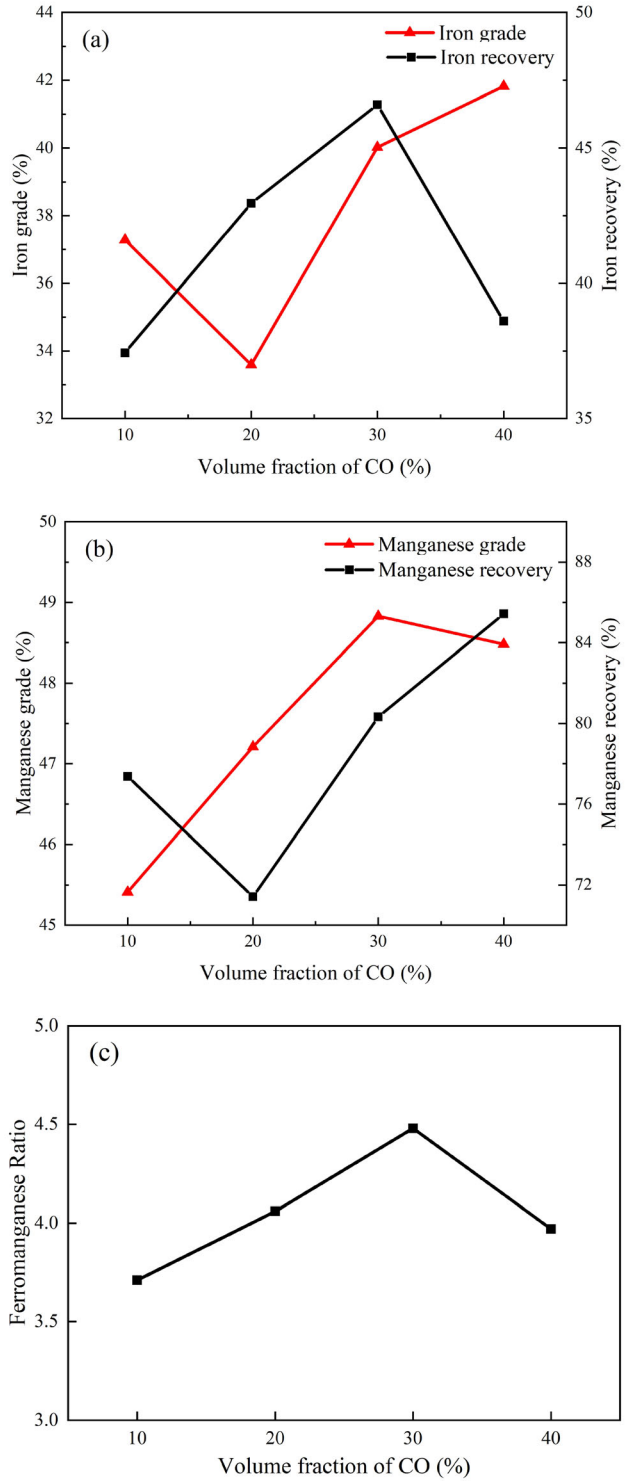

Fig. 9. Influence of CO concentration on roasting of manganese oxide ore: (a) iron concentrate; (b) manganese separation; (c) ratio of manganese to iron.

and manganese recovery of the manganese concentrate were 48.83% and 80.33%, and the manganese-to-iron ratio increased from 3.99 to 4.48. Considering the recovery of iron and manganese separation, the appropriate CO content was determined to be 30%.

Magnetic Separation Experiments

The liberation degree of target minerals in the ore has a significant impact on the quality of magnetic separation products. Due to the inability of direct roughing and scavenging to effectively separate manganese and iron, improving the grade and manganese iron ratio of the manganese concentrate by optimizing the grinding fineness was planned to improve the beneficiation effect. The effect of grinding fineness on the magnetic separation effect of manganese and iron synchronous reduction products is shown in Fig. 10 under the conditions of 750°C roasting temperature, 40 min roasting time, 30% CO concentration and 28.26 kA/m and 46.33 kA/m magnetic intensity of roughing and scavenging.

As shown in Fig. 10, the iron grade of the iron concentrate gradually increased with increasing grinding fineness, and the iron recovery rate decreased. The manganese grade of manganese concentrate decreased with the increase of grinding fineness, and the manganese recovery rate increased. Due to the relatively complete dissociation of individual particles with the increase of grinding fineness, the separation effect of regenerated magnetite was enhanced. However, if the particle size is too fine, some iron may not be recovered effectively. After comprehensive consideration, the grinding fineness of − 0.074 mm accounting for 82.56% was determined to be the appropriate grinding fineness. The iron grade and iron recovery of the magnetic concentrate were 40.30% and 58.73%, and the manganese grade and manganese recovery of the manganese concentrate were 48.95% and 72.50%. The manganese-to-iron ratio increased to 5.92. Even without using strong magnetic separation, effective separation and enrichment effects can be achieved.

Phase Transition Analysis

To study the valence states and existing forms of iron oxide and manganese oxide in roasted products at different roasting temperatures under gas-based roasting conditions, XRD and relative content analyses of manganese oxide and iron oxide were performed. The results are shown in Fig. 11.

Figure 11 shows the peak intensity and peak area of Mn_2O_3 and Fe_2O_3 gradually weakened with increasing roasting temperature, indicating they were gradually reduced, while the peak intensity of MnO and Fe_3O_4 gradually increased with the increase of roasting temperature. Based on the above thermodynamic analysis results, Mn_2O_3 and Fe_2O_3 were reduced to MnO and Fe_3O_4 with increasing roasting temperature. The temperature started from 650°C, and magnetite gradually formed. When the temperature exceeded 800°C, the Fe_2O_3 peak basically disappeared. The occurrence forms of iron oxides were primarily Fe_3O_4 and ferromanganese oxide. When roasting at 850°C,

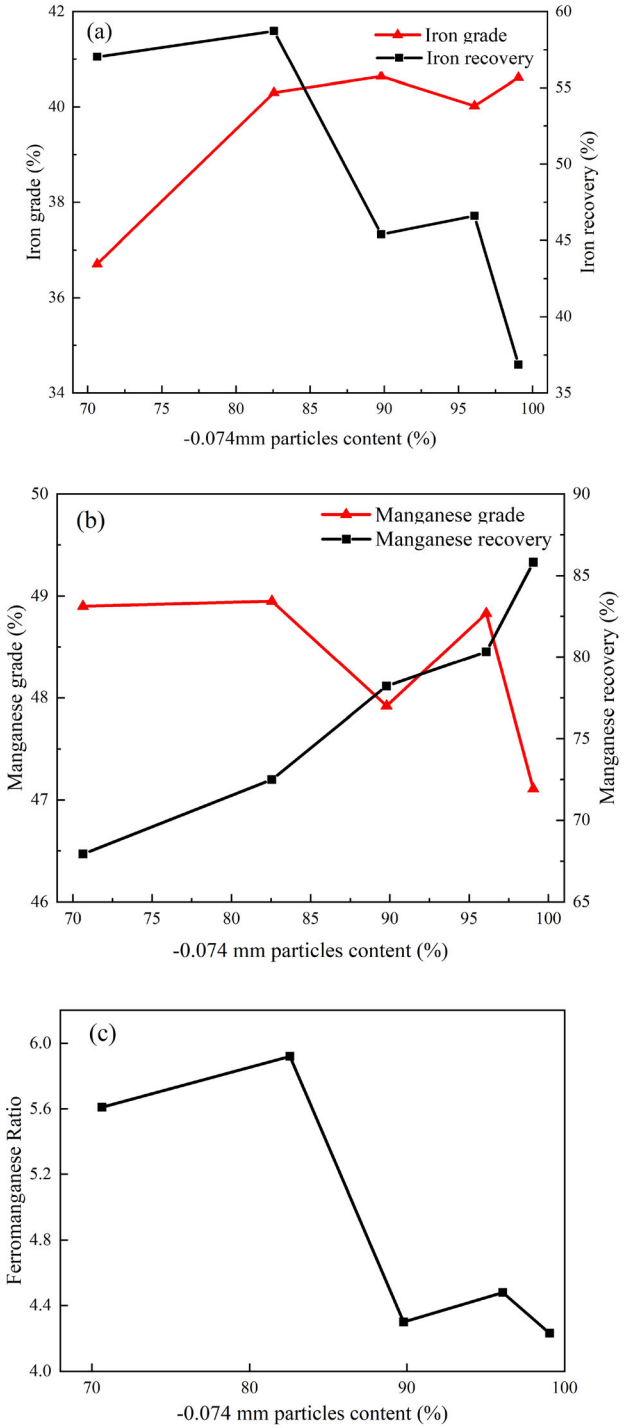

Fig. 10. Influence of grinding fineness on roasting of manganese oxide ore: (a) iron concentrate; (b) manganese product; (c) ratio of manganese to iron.

some Mn_2O_3 peaks still existed, indicating that manganese oxide did not transform into bivalent manganese completely. When roasting at 750°C, the relative content of magnetite in roasted products was the highest. When the roasting temperature was > 750°C, the relative content of magnetite decreased. The reason for this phenomenon was

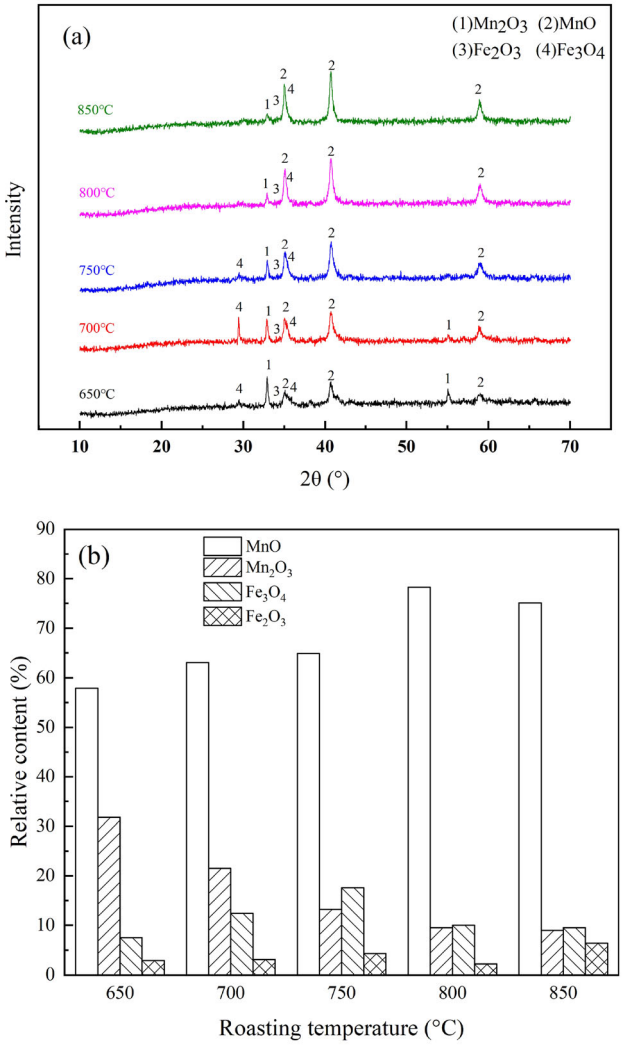

Fig. 11. Results of XRD analysis and relative content of manganese oxide and iron oxide in roasted products at different roasting temperatures: (a) XRD spectrum of gas-based roasted ore at different roasting temperatures; (b) relative content of iron and manganese oxides in gas-based roasted ore at different roasting temperatures.

probably the formation of wüstite or ferromanganese oxide due to the high temperature, resulting in the poor separation effect of manganese and iron. The magnetic separation test also showed that roasted products had the best separation effect between manganese and iron at a roasting temperature of 750°C. A large amount of unreduced hematite entering the tailings of magnetic separation of the roasted ore also resulted in the poor separation results at a roasting temperature of 650°C and 700°C.

XRD analysis of roasted products and relative content analysis of manganese oxides and iron oxides were performed to determine the valence and existence of manganese oxides and iron oxides in roasted products at different roasting times under gas-based conditions. The results are shown in Fig. 12.

From Fig. 12, the peak intensity and peak area of Mn_2O_3 and Fe_2O_3 gradually decreased with prolonged roasting time. The peaks of Mn_2O_3 and Fe_2O_3 gradually disappeared and the relative content of Mn_2O_3 and Fe_2O_3 gradually decreased when the roasting time exceeded 60 min. The peak intensity and area of MnO and Fe_3O_4 in the roasted products gradually increased when the roasting time was prolonged from 20 min, and the relative content of MnO and Fe_3O_4 gradually increased. The transformation trend was accelerated when the roasting time was > 40 min, consistent with the previous magnetic separation test results. Some Fe_3O_4 diffraction peaks weakened when the roasting time exceeded 80 min, indicating that excessive roasting time might lead to overreduction reactions of iron oxides and result in poor separation of iron and manganese.

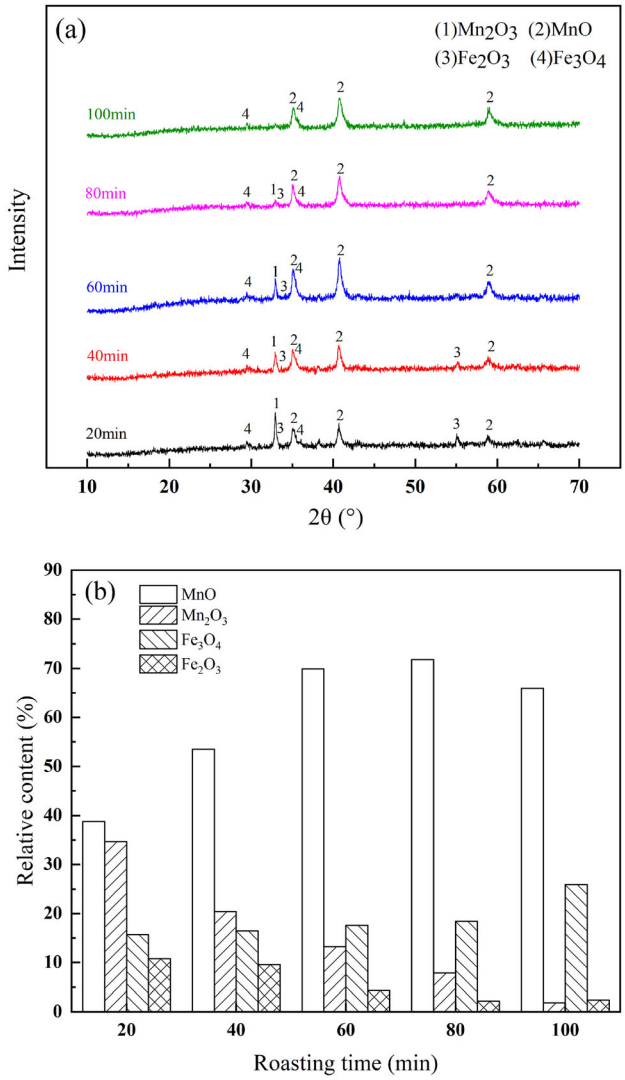

Fig. 12. Results of XRD analysis and relative content of manganese oxide and iron oxide in roasted products at different roasting times: (a) XRD spectrum of gas-based roasted ore at different roasting times; (b) relative content of iron and manganese oxides in gas-based roasted ore at different roasting times.

SEM Mapping Analysis

SEM-EDS analysis was conducted to study the microstructure changes of the reduction roasting products of the ferromanganese ore at different roasting temperatures. The SEM-EDS analysis results are exhibited in Fig. 13.

Figure 13a shows that Fe_2O_3, Mn_2O_3 and trace amounts of manganese-iron oxide in the raw ore were decomposed and reduced at a roasting temperature of 650°C, partially converted into Fe_3O_4 and MnO. Fe_3O_4 was generated in the bright gray area of the color edge, and the contents of Ca, Si and Al in the gray-brown area were higher based on the previous XRD analyses, indicating a trend of aggregation.

Figure 13c shows that the trend that Fe_2O_3 and Mn_2O_3 in the raw ore converted into Fe_3O_4 and MnO and further expanded under the reduction conditions of 750°C roasting temperature. The crystals of iron and manganese oxides were denser, and the boundary area of oxide grains was also more obvious.[30] Because the newly generated MnO and Fe_3O_4 crystal forms were more perfect at 750°C, the comprehensive recovery of manganese and iron in grinding and separation was improved based on the previous XRD phase composition and relative content analysis. The grains of Ca, Si and Al in the grayish brown area had a tendency to further aggregate, and they might aggregate with manganese oxides, possibly separating into non-magnetic product manganese concentrates.

According to the SEM-EDS analysis of roasted ore (Fig. 13e) and XRD analysis, Mn_2O_3 completely transformed into MnO when the roasting temperature was 850°C, and the iron phase was primarily the regenerated magnetite outside the particles and the unreduced hematite inside the larger particles. Some small particles were overreduced to produce wüstite.[31] The bright gray areas in the figure were magnetite and wüstite, and the relatively dark iron oxide particles were hematite. Compared with the roasting ore at 800°C, the impurity elements were further migrated and gathered together, and the particle size tended to increase, indicating that high temperature was conducive to the aggregation of Ca, Si and Al oxides.

CONCLUSION

(1) The appropriate conditions for gas-based roasting were 750°C roasting temperature, 40 min roasting time and 30% CO volume fraction. After the roasted ore was processed by low intensity magnetic separation, the iron grade and iron recovery of the iron concentrate were 40.30% and 58.73%; the manganese grade and manganese recovery of the manganese concentrate product were 48.95% and

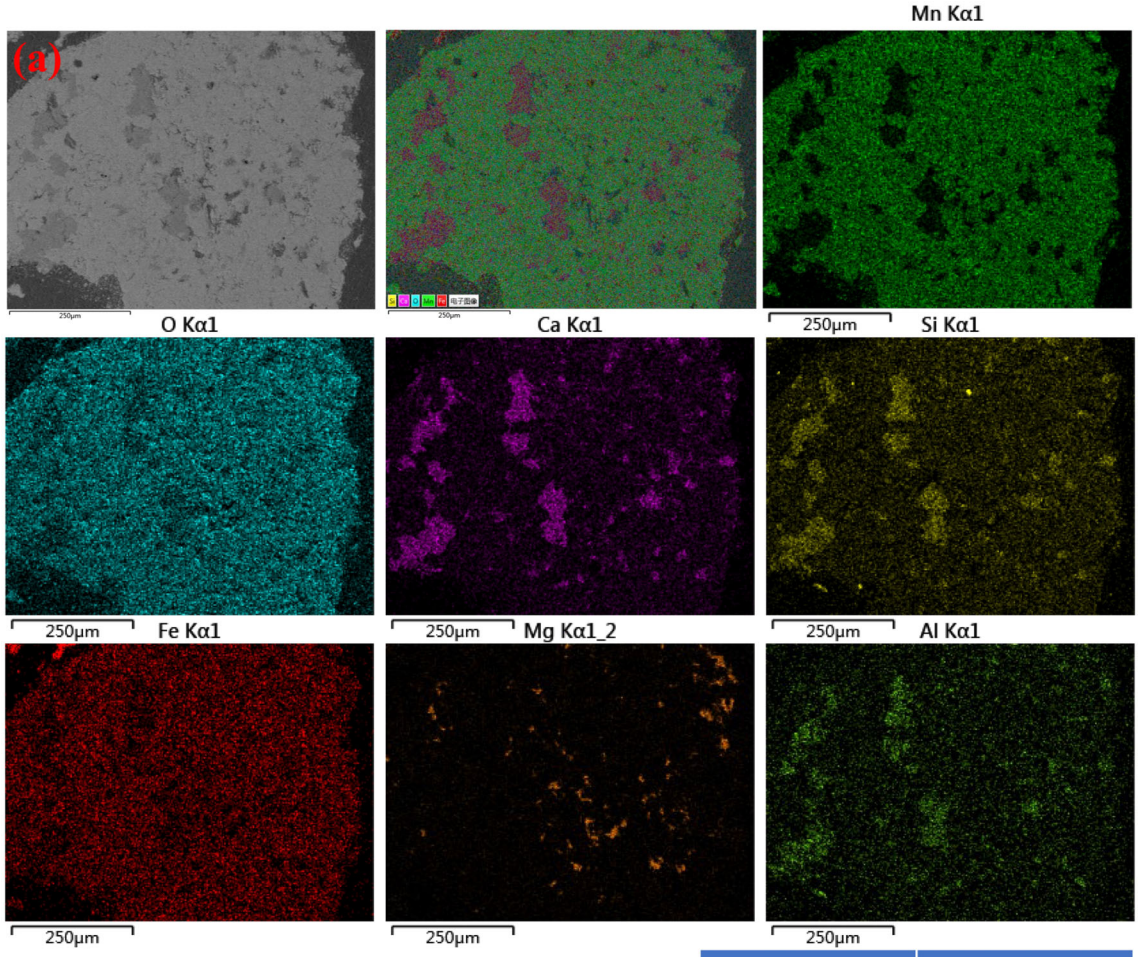

Element	Atomic percent / %
O	47.18
Mn	31.93
Fe	7.14
Si	5.41
Ca	6.05
Mg	1.77
Al	0.53
Total	100.00

Fig. 13. SEM mapping of roasted ore under different roasting temperatures: (a) 650°C; (b) 700°C; (c) 750°C; (d) 800°C; (e) 850°C.

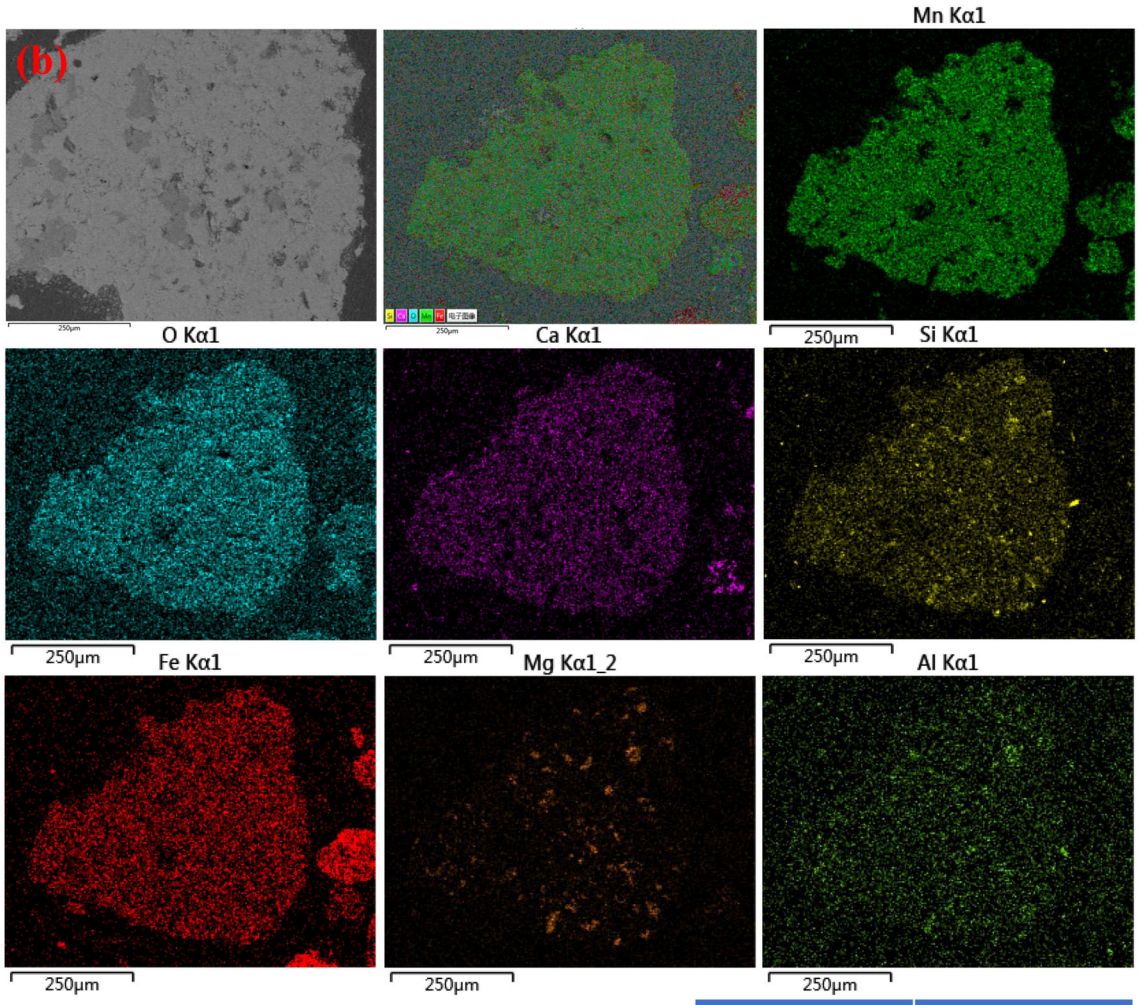

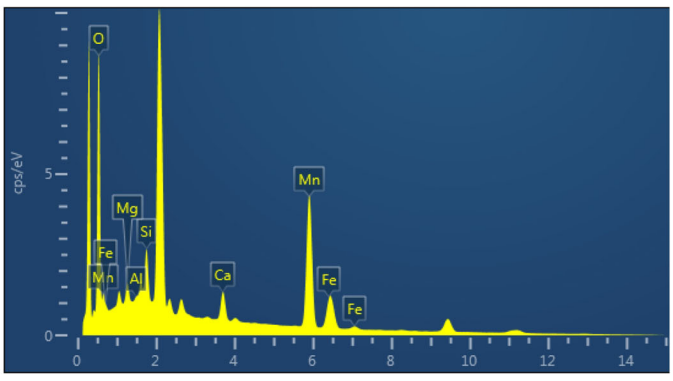

Element	Atomic percent / %
O	46.27
Mn	35.29
Fe	7.67
Si	4.81
Ca	3.34
Mg	2.62
Al	0.00
Total	100.00

Fig. 13. continued

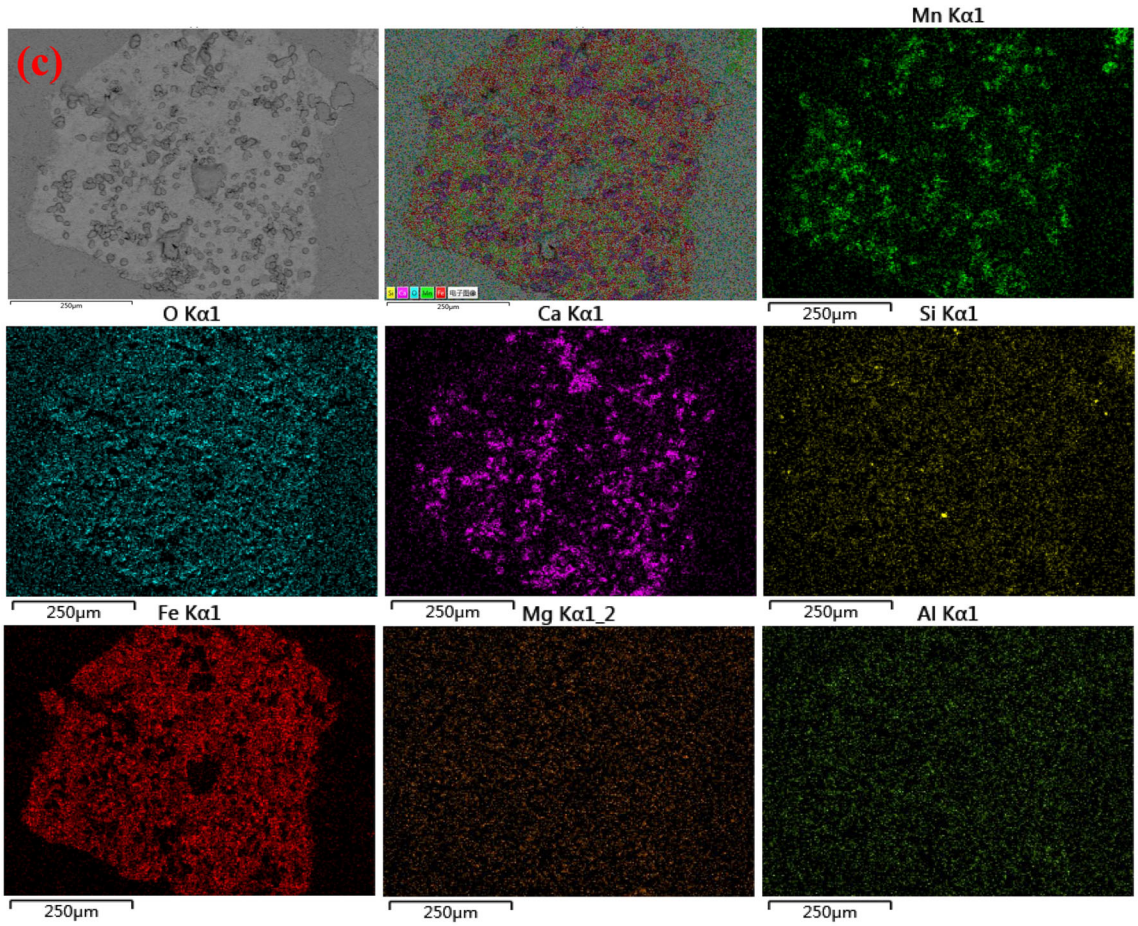

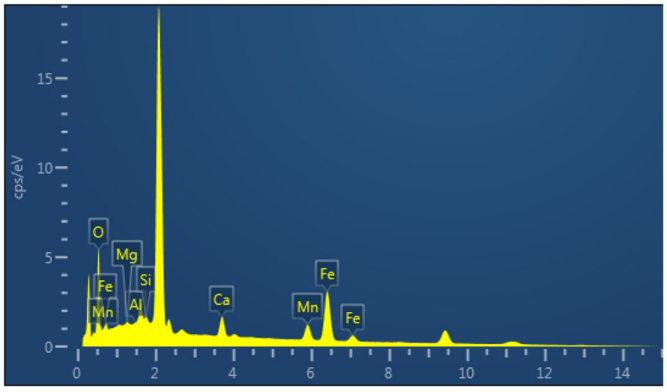

Element	Atomic percent / %
O	42.59
Mn	10.06
Fe	39.00
Si	1.53
Ca	5.82
Mg	1.00
Al	0.00
Total	100.00

Fig. 13. continued

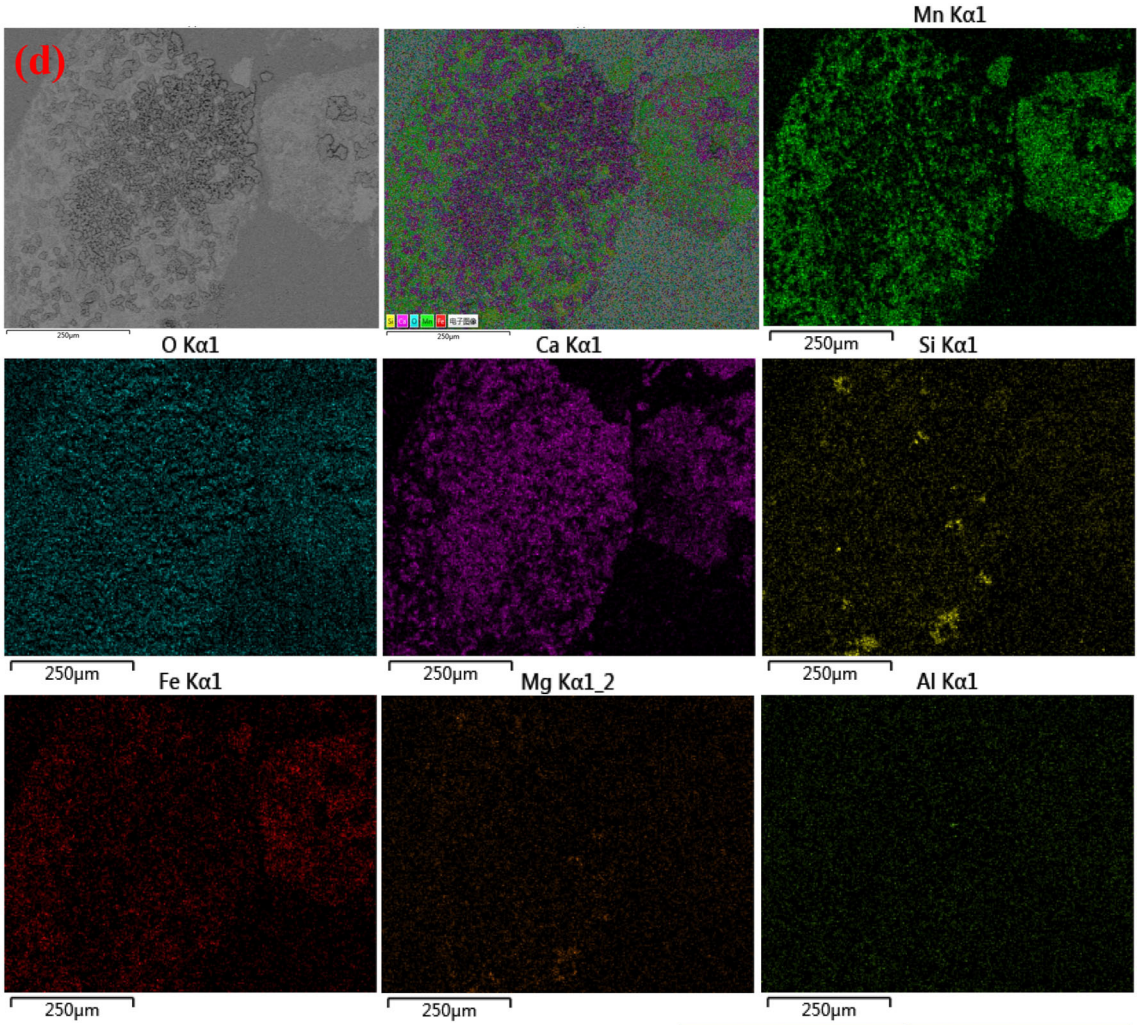

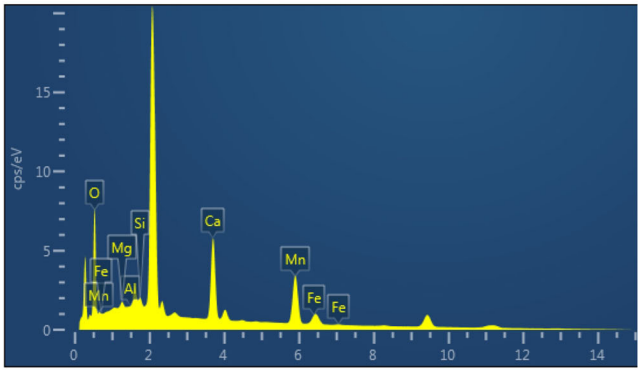

Element	Atomic percent / %
O	55.02
Mn	22.37
Fe	3.84
Si	1.30
Ca	16.31
Mg	1.16
Al	0.00
Total	100.00

Fig. 13. continued

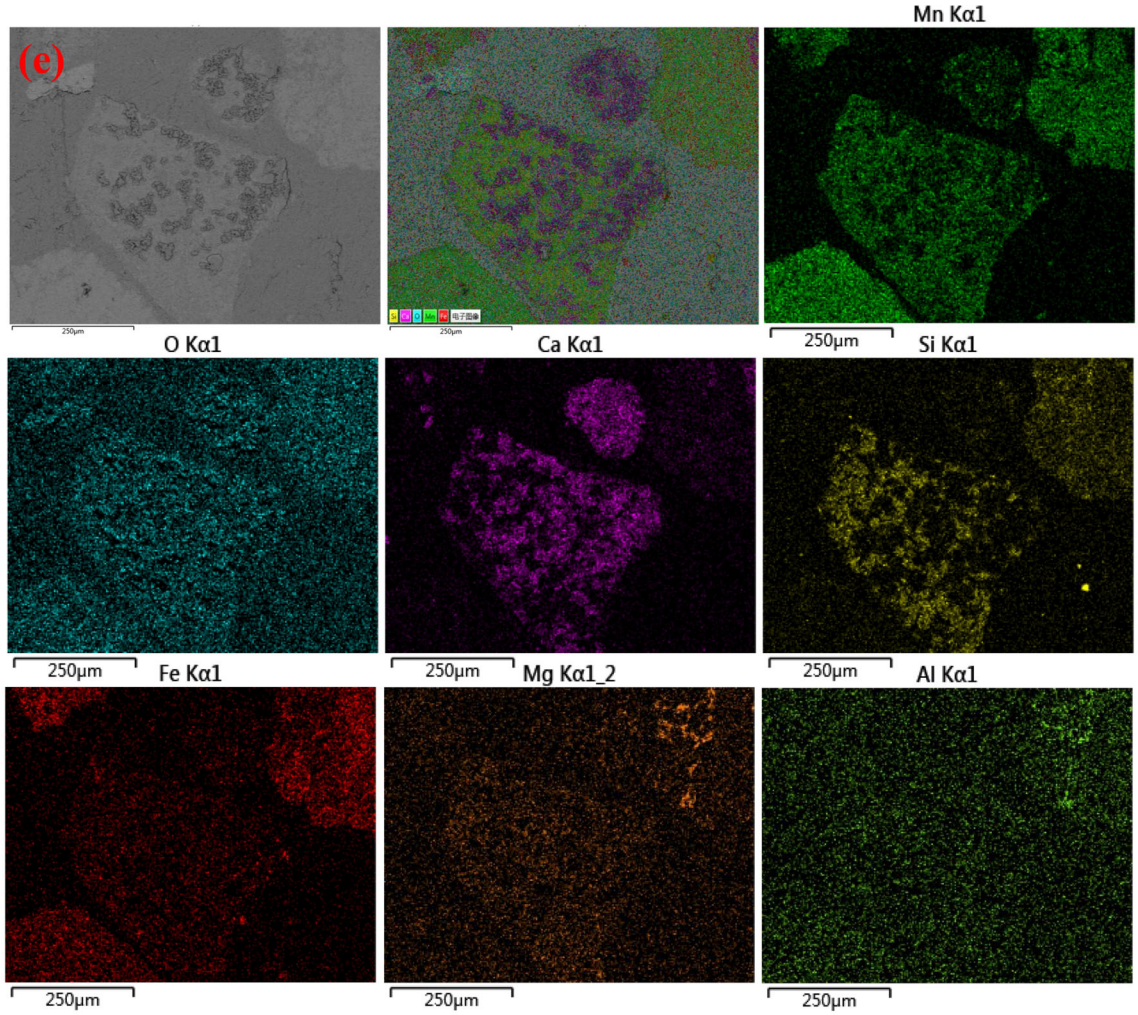

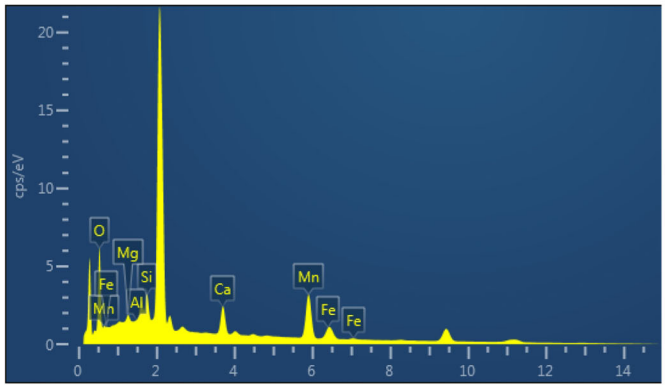

Element	Atomic percent / %
O	46.82
Mn	29.43
Fe	7.30
Si	5.88
Ca	8.35
Mg	2.22
Al	0.00
Total	100.00

Fig. 13. continued

72.50%, with the manganese-to-iron ratio increasing from 2.5 to 5.92.

(2) Mn_2O_3 and Fe_2O_3 gradually reduced to MnO and Fe_3O_4 with the increase of temperature, during the magnetization reduction process of iron-rich manganese oxide ore. Iron oxide and manganese oxide could basically achieve synchronous reduction when CO was used as a reducing agent and roasting at 750°C. Overreduction reactions might occur when the temperature exceeded 800°C. Under gas-based conditions, Mn_2O_3 was directly reduced to form MnO under gas-based conditions, without generating the intermediate product Mn_3O_4.

(3) Compared with the roasting temperature of 650°C, the crystals of iron and manganese oxides were denser, and the grains of Ca, Si and Al had a tendency to further aggregate at a roasting temperature of 750°C. Mn_2O_3 completely transformed into MnO when the roasting temperature was 850°C, and the iron phase was primarily the regenerated magnetite outside the particles and the unreduced hematite inside the larger particles. The impurity elements migrated further and gathered together at 850°C roasting temperature, indicating that the crystal forms of MnO and Fe_3O_4 were more perfect and the coexisting grains of Ca, Si and Al clustered further with the roasting temperature increasing.

ACKNOWLEDGEMENTS

The authors are grateful to the National Natural Science Foundation of China (Grant Nos. 51974204 and 52204276) and Key R&D Plan Projects in Hubei Province (Grant No. 2022BCA062).

CONFLICT OF INTEREST

The authors declare that they have no conflict of interest.

REFERENCES

1. T. Coetsee, *Miner. Process Technol. Rev.* 39, 351 (2018).
2. X. Wang, G.J. Xie, N. Tian, C.C. Dang, C. Cai, J. Ding, B.F. Liu, D.F. Xing, N.Q. Ren, and Q.L. Qi, *Sci. Total. Environ.* 822, 153513 (2022).
3. M. Wang, X. Zheng, X. Zhang, D.L. Chao, S.Z. Qiao, H.N. Alshareef, Y. Cui, and W. Chen, *Adv. Energy Mater.* 11, 2002904 (2021).
4. R.R. Zhang, X.T. Ma, X.X. Shen, Y.J. Zhai, T.Z. Zhang, C.X. Ji, and J.L. Hong, *J. Clean. Prod.* 253, 119951 (2020).
5. J. Xing, L. Hou, H. Du, B.S. Liu, and Y.H. Wei, *JOM* 71, 4715 (2019).
6. Y. Du, X.H. Gao, Z.W. Du, Y. Dong, B. Zhang, R.D.K. Misra, H.Y. Wu, and L.X. Du, *JOM* 73, 3301 (2021).
7. F. He, J. Chen, G. Chen, J.H. Peng, C. Srinivasakannan, and R. Ruan, *JOM* 71, 3909 (2019).
8. D. He, J. Shu, R. Wang, M.J. Chen, R. Wang, Y.S. Gao, R.L. Liu, Z.H. Liu, Z.H. Xu, D.Y. Tan, H.N. Gui, and N. Wang, *J. Hazard. Mater.* 418, 126235 (2021).
9. J. Ju, Y. Feng, H. Li, and X.F. Zhong, *JOM* 74, 1978 (2022).
10. B. Liu, Y. Zhang, M. Lu, Z.J. Su, G.G. Li, and T. Jing, *Miner. Eng.* 131, 286 (2019).
11. J. Hu, L. Chen, J.L. Zhang, Y. Zhou, J. Zhang, L.W. Cao, W.J. Zhao, H.L. Tao, J.K. Yang, and F.F. Wu, *JOM* 75, 3511 (2023).
12. F. Teng, S. Luo, W. Mu, X.F. Lei, H.X. Xin, Y.C. Zhai, and Y.N. Nian, *JOM* 70, 2008 (2018).
13. V. Singh, K.V. Reddy, S.K. Tripathy, P. Kumari, A.K. Dubey, R. Mohanty, R.R. Satpathy, and S. Mukherjee, *J. Clean. Prod.* 284, 124784 (2021).
14. V. Singh, T. Chakraborty, and S.K. Tripathy, *Miner. Process. Extr. Metall. Rev.* 41, 417 (2020).
15. A. Cheraghi, H. Yoozbashizadeh, and J. Safarian, *Miner. Process. Extr. Metall. Rev.* 41, 198 (2020).
16. F. Teng, S.H. Luo, W.N. Mu, X.F. Lei, H.X. Xin, Y.C. Zhai, and Y.N. Dai, *JOM* 70, 2008 (2018).
17. X. Cai, F. Shen, Y. Zhang, H.Y. Hu, Z.Q. Huang, Y.Z. Yin, X.T. Liang, Y.B. Qin, and J. Liang, *J. Hazard. Mater.* 366, 466 (2019).
18. J. Du, L. Gao, Y. Yang, S.H. Guo, J. Chen, M. Omran, and G. Chen, *Adv. Powder Technol.* 31, 2901 (2020).
19. Y. Zhang, Y. Zhao, Z. You, D.X. Duan, G.H. Li, T. Jiang, and J. Cent, *South Univ.* 22, 2515 (2015).
20. Y. Gao, H.G. Kim, H.Y. Sohn, and C.W. Kim, *ISIJ Int.* 52, 759 (2012).
21. L. Qin, W. Wu, X. Cheng, F. Xu, and X. Li, *JOM* 75, 2212 (2023).
22. B. Liu, Y. Zhang, J. Wang, J. Wang, Z.J. Su, G.H. Li, and T. Jiang, *Adv. Powder Technol.* 30, 302 (2019).
23. W. Li, G.Q. Fu, M.S. Chu, and M.Y. Zhu, *J. Iron. Steel Res. Int.* 24, 34 (2017).
24. H. Zhang, P. Zhang, F. Zhou, and M. Lu, *Int. J. Min. Sci. Technol.* 32, 865 (2022).
25. K. Quast, *Miner. Eng.* 126, 89 (2018).
26. V.P. Ponomar, O.B. Brik, Y.I. Cherevko, and V.V. Ovsienko, *Chem. Eng. Res. Des.* 148, 393 (2019).
27. S.K. Roy, D. Nayak, and S.S. Rath, *Powder Technol.* 367, 796 (2020).
28. P. Liu, X. Zhu, Y. Han, Y.J. Li, and P. Gao, *Powder Technol.* 414, 118107 (2023).
29. S. Yuan, R. Wang, P. Gao, Y. Han, and Y. Li, *Powder Technol.* 396, 80 (2022).
30. Z. Wang, Z. Yang, L. Liu, Y.P. Ye, and X.Y. Xie, *Sep. Purif. Technol.* 302, 122107 (2022).
31. I. Castellanos-Rubio, I. Rodrigo, R. Munshi, O. Arriortua, J. Garitaonandia, A. Martinez-Amesti, F. Plazaola, I. Orue, A. Pralle, and M. Insausti, *Nanoscale* 11, 16635 (2019).